International Journal of Applied Pharmaceutics

ISSN- 0975-7058 Vol 16, Issue 6, 2024

Original Article

DESIGN, SYNTHESIS, AND BIO PROFILING OF 2, 3-DIHYDROQUINAZOLIN-4(1H)-ONE DERIVATIVE AS TYPE II DIABETES AGENTS: A COMPREHENSIVE *IN SILICO, IN VITRO*, AND *IN VIVO* STUDY

MINCY MATHEW[1*], D. KILIMOZHI[2], SANTHOSH M. MATHEWS[3], A. ANTON SMITH[4]

[*1,2,4]Department of Pharmacy, Faculty of Engineering and Technology, Annamalai University, Tamilnadu, India. [3]Department of Pharmaceutics, Pushpagiri College of Pharmacy, Kerala, India

[*]Corresponding author: Mincy Mathew; [*]Email: min_cmath@yahoo.co.in

Received: 05 Jun 2024, Revised and Accepted: 16 Sep 2024

ABSTRACT

Objective: Diabetes mellitus is a significant global health challenge, with Type 2 Diabetes Mellitus (T2DM) being a leading cause of mortality worldwide, demanding the need for effective interventions by developing innovative therapeutic strategies or novel antidiabetic agents. This study explores *in silico*, *in vitro*, and *in vivo* approaches to identify the most potent 2,3-Dihydroquinazolin-4(1H)-One derivative molecule with antidiabetic activity.

Methods: Eleven new derivatives were designed, studied *in silico* to identify the most promising compounds, synthesized, studied spectrally to describe them, and evaluated for both *in vitro* and *in vivo* investigations. Alpha amylase and alpha-glucosidase inhibitory activities were investigated *in vitro*. The endogenous suppression of glucose synthesis in Hepatoblastoma cell line 2(HepG2) cells and the *in vitro* glucose absorption assay on cultivated L6 cell lines were conducted. To assess the ability of the newly synthesized compounds to prevent diabetes, *in vivo* investigations were conducted on Streptozotocin (STZ)-induced diabetic rats and the effects on various biochemical parameters were identified.

Results: Leveraging computational methods, the QZ9 molecule was identified with stable interactions with key biomolecules associated with T2DM. Subsequent *in vitro* assays confirmed the inhibitory effects of QZ2, QZ8, and QZ9 on alpha-amylase and alpha-glucosidase activities, suggesting their potential as enzyme inhibitors. Additionally, QZ8 and QZ9 demonstrated enhanced glucose uptake and production inhibition in HepG2 cells, indicating their role in improving glucose homeostasis. *In vitro,* the top-ranked molecules QZ2, QZ8, and QZ9 were analyzed to validate the *in silico* findings and assess their potential as therapeutic agents for T2DM. The inhibition of α-amylase activity by QZ2, QZ8, and QZ9 was dose-dependent, with maximum inhibition observed at 1000 µg/ml: 57.33% for QZ2, 52.21% for QZ8, and 87.16% for QZ9. Similarly, α-glucosidase inhibition at 1000 µg/ml was 59.96% for QZ2, 53.50% for QZ8, and 81.51% for QZ9. Both QZ8 and QZ9 significantly increased glucose uptake and inhibited glucose production in HepG2 cells, with maximum glucose production inhibition at 100 µg/ml: 62.22% for QZ8 and 62.35% for QZ9. These findings suggest that QZ8 and QZ9 contribute to glucose homeostasis. QZ9 demonstrated superior enzyme inhibition compared to QZ2 and QZ8, with α-amylase and α-glucosidase inhibition up to 87.16% and 81.51%, respectively, at 1000 µg/ml. In vivo investigations in Diabetic rat models further confirmed the efficacy of these compounds by showing significant reductions in blood glucose levels. These results suggests the potentiality of QZ9 as a promising novel Antidiabetic agent.

Conclusion: Combining computational predictions with experimental validations, this integrated approach highlights the promise of 2,3-Dihydroquinazolin-4(1H)-One derivative QZ9 as a novel antidiabetic agent, warranting further investigation for clinical translation.

Keywords: Diabetes mellitus, Type 2 diabetes mellitus, Antidiabetic, Drug design, 2,3-Dihydroquinazolin-4(1H)-One

DOI: https://dx.doi.org/10.22159/ijap.2024v16i6.51705 Journal homepage: https://innovareacademics.in/journals/index.php/ijap

INTRODUCTION

Diabetes mellitus, characterized by hyperglycemia, has emerged as a global health concern with escalating prevalence, particularly in countries such as India [1]. The staggering projections for the rise in diabetes cases underscore the urgent need for effective interventions. Due to its multiorgan consequences and substantial global mortality rate, type 2 diabetes mellitus (T2DM) calls for further study to develop better treatment approaches. Maintaining optimal glucose, lipids, and pressure levels in the blood is significant in delaying diabetes-related complications [2]. Several biomolecules, including alpha-amylase, insulin-like growth factor 1 receptor, sulfonylurea receptor-1, glycogen phosphorylase, lysosomal acid-alpha-glucosidase, glycogen synthase kinase-3 beta, dipeptidyl peptidase, and PPAR-γ, play pivotal roles in the intricate network of mechanisms related to diabetes and insulin production/balancing in the human body [3].

Various natural and synthetic heterocyclic compounds possess antidiabetic activity. Thiazolidinone, pyrrole, azole, pyrimidine, chalcone, etc. are fundamental structural scaffolds for these pharmacologically active compounds. Various categories of drugs practice different mechanisms to regulate blood glucose levels [4]. Nevertheless, synthetic medications are consistently linked with numerous adverse reactions. Therefore, it is crucial to investigate new lead molecules with better efficacy to treat diabetes and minimize side effects. Quinazolinone is a heterocyclic ring structure containing nitrogen, which is linked to various therapeutical features such as anticancer, antimalarial, anticonvulsant, anti-inflammatory, antibacterial, antifungal, hypolipidemic and antidiabetic characteristics. In the pursuit of novel antidiabetic agents, the study focuses on 2,3-dihydroquinazolin-4(1H)-one derivative [5-8].

The research aims to address the limitations of existing synthetic drugs by exploring compounds with improved efficacy and reduced side effects. Traditional drug discovery processes are time-consuming, prompting the adoption of computational drug discovery as a cost-effective alternative. This study employs *in silico, in vitro*, and *in vivo* studies to accelerate the discovery of novel molecules with antidiabetic properties, reducing reliance on resource-intensive laboratory experiments. For the *in silico* phase, modelled 2,3-dihydroquinazolin-4(1H)-one analogue are considered as ligands to target the biomolecules such as alpha-amylase, insulin-like growth factor 1 receptor, sulfonylurea receptor-1, glycogen phosphorylase, lysosomal acid-alpha-glucosidase, glycogen synthase kinase-3 beta, dipeptidyl peptidase, and peroxisome proliferator-activated receptor gamma.

Moving beyond *in silico* predictions, the research integrates *in vitro* studies to validate the potential antidiabetic activity. It incorporates

various inhibitory assays, including α-amylase, α-glucosidase, glucose production in the liver, and determination of glucose absorption assay in cultured L6 Cell Lines. The *in vivo* study comprises determining blood glucose level, Histopathology study, Lipid profile, etc. This comprehensive approach aims to narrow the disparity between computational predictions and real-world efficacy, bringing us closer to the development of effective and safe antidiabetic agents.

MATERIALS AND METHODS

Chemicals and reagents used for the study

All the chemicals and reagents used in the research were of AR grade. It includes Isatoic anhydride, Hydrazine hydrate, p-hydroxy benzaldehyde, 2,4-dimethoxy benzaldehyde and 3,4 dimethoxy benzaldehyde supplied from TCI, Japan. Alum, Ethyl acetate, n-hexane, Dimethyl Formamide, Methanol, Acetone, Chloroform, Potassium Dihydrogen Phosphate, Sodium Hydroxide, α-glucosidase, Sodium carbonate, Glucagon, Nicotinamide from Sigma-Aldrich, Mumbai. α-Amylase, 3,5-Dinitro salicylic acid, Sucrose, TrisHCl, Sodium Chloride, Triton purchased from Himedia Laboratories. Glucose Reagent and Glucose Kit (Coral Clinical System), DMEM (Gibco), Trypsin and EDTA ((Invitrogen), Streptozotocin (Merck) and SGOT Kit, SGPT Kit and ALP Kit (Erba Manheim) were also used in this research work.

In silico analysis

We employed various computational tools to evaluate the drug ability of the proposed ligand molecules in this study. Softwares/tools such as ACD/ChemSketch for structure drawing, Avogadro for modelling 11 (QZ1 to QZ11) 2,3-dihydroquinazolin-4(1H)–one derivative molecule, Molinspiration Cheminformatics, Swiss ADME [9], PkCSM [10], and OSIRIS Property Explorer software were employed to calculate the molecular, ADMET (Absorption, Distribution, Metabolism, Excretion, and Toxicity) properties and screening for drug-like qualities. Molecular interaction analysis between targets and ligand molecules was performed using AutodockVina software (v.1.2.0.) [11, 12], to predict binding affinity and interaction conformation of considered ligands with receptors. The selected targets, including alpha-amylase (Protein Data Bank (PDB) ID: 1B2Y)[13,14], Insulin-like growth factor 1 receptor (PDB ID: 2OJ9) [15], sulfonylurea receptor-1 (PDB ID: 6JB3) [16], glycogen phosphorylase (PDB ID: 3DD1)[17], lysosomal acid-alpha-glucosidase (PDB ID: 5NN8) [18], glycogen synthase kinase-3 beta (PDB ID: 1UV5) [19], dipeptidyl peptidase (PDB ID: 4CDC) [20], and peroxisome proliferator-activated receptor gamma (PDB ID: 4PRG) [21], were subjected to molecular docking with both the modelled molecules and their corresponding standard drug molecules. Discovery Studio Biovia 2017 (DS) visualizer aided interaction analysis and Molecular Dynamic (MD) Simulation in GROMACS validated stability [22, 23]. Trajectory plots and interaction analysis were performed, assessing parameters like Root mean Square Deviation (RMSD), Root mean Square Fluctuation (RMSF), Radius of Gyration (RoG), H-bond interaction distribution, and Solvent Accessible Surface Area (SASA) using Xmgrace. Visualization of complexes and interactions utilized DS Visualizer, Visual Molecular Dynamics (VMD), and Pymol. The gmx_MMPBSA (Molecular Mechanics Poisson-Boltzmann Surface Area) M package in GROMACS software was utilized to perform MMPBSA calculations [24].

Preparation of 2,3-dihydroquinazolin-4(1H)–one derivative

Standard protocol

A combination of 1 mmol isatoic anhydride, 1 mmol hydrazine hydrate, and various benzaldehyde derivative (2 mmol) was prepared in 5 ml ethanol. Subsequently, solution, 0.4 mmol alum was introduced into the solution, followed by refluxing the mixture for 5 h at 78 °C. Upon culmination of the reaction, validated through thin-layer chromatography (TLC), the catalyst was removed through filtration. The resulting filtrate was combined with 10 ml of water to induce precipitation. The precipitate obtained was subjected to filtration and further purified through recrystallization in ethanol [25, 26]. The scheme of the reaction and the plausible mechanism were shown in Scheme: 1 and Scheme: 2, respectively.

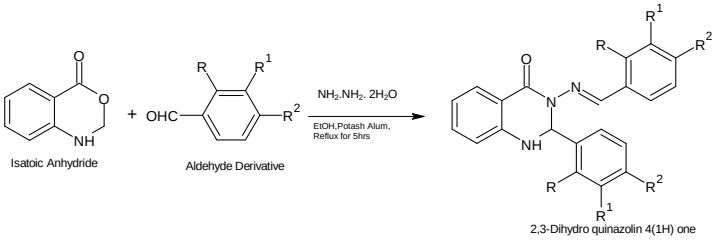

Derivative	R	R1	R2
Qz2	H	H	OH
Qz8	OCH3	H	OCH3
Qz9	H	OCH3	OCH3

Scheme 1: Scheme of reaction for the synthesis of 2,3-dihydroquinazolin-4(1H)–one derivative

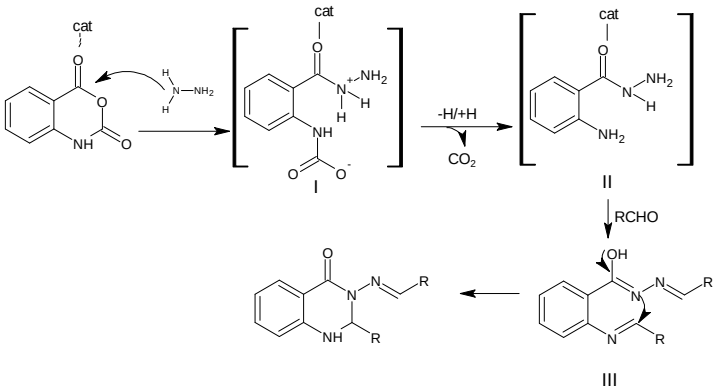

Scheme 2:-Plausible mechanism of the reaction

The catalyst facilitates the nucleophilic attack on the carbonyl carbon of the isatoic anhydride. Nucleophilic addition leads to intermediate I followed by the elimination of carbon dioxide produces the structure anthranilamide II. The catalyst promotes the nucleophilic attack of the amino groups of II on the carbonyl carbon of the aldehyde, resulting in the formation of the Schiff base III. Finally, the imine intramolecularly cyclizes by nucleophilic attack of the nitrogen on the imine carbon to produce the corresponding Dihydroquinazoline derivative [27].

Preparation of 2-(4-hydroxyphenyl)-3-{(E)-[(4-hydroxyphenyl) methylidene] amino}-2,3-dihydroquinazolin-4(1H)-one (QZ2)

Same procedure was followed for preparation of 2-(4-hydroxyphenyl)-3-{(E)-[(4-hydroxyphenyl) methylidene] amino}-2,3-dihydroquinazolin-4(1H)-one with p-hydroxy benzaldehyde as aldehyde derivative. $C_{21}H_{17}N_3O_3$, whitish solid m. p: 186°-190 °C, Rf 0.23(n-Hexane: Ethyl acetate,6:4),IR(ATR,cm^{-1}) 3160 (Ar-OH), 3319(NH), 2920(Ar-CH) 1233(C-O), 1603(C=O) 1598(C-N) ^{1}HNMR (400MHz, DMSO-d6,ppm) 6.25-6.5 (1H, CH) 6.75-7.5 (12H, ArH) 7.5-8 (2H, OH) 8.5-8.75(2H,NH,=CH)[13]CNMR70-80(C8)110-.115 (C16, C18, C22, C24) 118.29 (C5, C3) 126 (C1) 128.65 (C25, C14,C6) 130-135 (C19, C20,C15) 134.41 (C2)145-150 (C4-C13)158.65(C23, C17) 165.97(C10) LC-MS(70ev,m/z)360[M+].

Preparation of 2-(2,4-dimethoxyphenyl)-3-{(E)-[(2,4-dimethoxyphenyl) methylidene] amino}-2,3-dihydroquinazolin-4(1H)-one (QZ8)

The same procedure was followed for preparation of 2-(2,4-dimethoxyphenyl)-3-{(E)-[(2,4-dimethoxyphenyl) methylidene] amino}-2,3-dihydroquinazolin-4(1H)-one with 2,4-dimethoxy benzaldehyde as aldehyde derivative. $C_{25}H_{25}N_3O_5$, off-white solid m. p: 168°-170 °C,Rf 0.86(n-Hexane: Ethyl acetate,6:4),IR(ATR,cm^{-1}) 3000,2975 (Ar-CH), 3348(NH), 1162(C-O-C) 1263(C-O), 1601(C=O) 1571 (ArC-C) ^{1}HNMR (400MHz, DMSO-d6,ppm)3.5-4(12H, OCH3) 6.25-6.5 (1H,CH) 6.5-7.75 (10H,ArH)8.5-8.75(2H,N-H,=CH)[13]CNMR50-60(4C)60-70(C8)95-.100(2C)105-110(2C)118.25 (2C) 123.9(C1) 127.10134.3 (3C) 146.7-152.3 (2C) 155-160 (4C)163.12 (C10) LC-MS(70ev,m/z) 448[M+].

Preparation of 2-(3,4-dimethoxyphenyl)-3-{(E)-[(3,4-dimethoxyphenyl) methylidene] amino}-2,3-dihydroquinazolin-4(1H)-one (QZ9)

Same procedure was followed for synthesis of 2-(3,4-dimethoxyphenyl)-3-{(E)-[(3,4-dimethoxyphenyl) methylidene] amino}-2,3-dihydroquinazolin-4(1H)-one with 3,4-dimethoxy benzaldehyde as aldehyde derivative. $C_{25}H_{25}N_3O_5$, off-white solid m. p: 162°-164 °C, Rf 0.62(n-Hexane: Ethylacetate,6:4) IR (ATR,cm^{-1}) 3195 (Ar-CH), 3480(NH), 1159(C-O-C) 1257(C-O), 1577(C=O) 1507(ArC-C) ^{1}HNMR (400MHz, DMSO-d6, ppm)3.5-4(12H, OCH3) 6.41 (1H, CH) 6.75-7.77 (10H, ArH) 8.5-8.75(2H, N-H,=CH)[13]CNMR 50-60(4C) 72.06 (C8)108.5-110.9(4C)115.2-118.9(2C) 122.5-123.4(3C) 13.5-134.5 (2C) 146.7-149.4 (2C) 151.03-152.3 (4C)161.29 (1C) LC-MS(70ev,m/z) 448[M+]

***In vitro* evaluations**

Alpha amylase inhibition assay

For the experimental procedure, various concentrations of the test sample ranged from 62.5µg/ml to 1000µg/ml, from a 10 mg/ml stock concentration. These samples were then combined with phosphate buffer (25 mmol, pH 6.9) and 25 units of porcine α-amylase at a density of 0.5 mg/ml. Incubation of these mixtures occurred at 25 °C for 10 min. Afterwards, 25 µl of a phosphate buffer (25 mmol, pH 6.9) containing a 0.5% starch solution was introduced, and the process combinations were once again incubated at 25 °C for an additional 10 min. The ensuing reactions were terminated by the addition of 50µl of a 96 mmol 3, 5-dinitrosalicylic acid colour reagent. Following this, the microplate was subjected to a 5 min incubation in a boiling water bath and then allowed to cool to room temperature. The absorbance of the resultant solution was assessed at 540 nm employing a microplate reader (Erba, Lisascan) [28]. The percentage of inhibition can be calculated using the formula:

$$\%\ of\ inhibition\ = \frac{control - test}{control} \times 100$$

Alpha-glucosidase inhibition assay

The experimental procedures closely followed the methodology outlined by Matsui *et al.* with minor adaptations. Samples of various concentrations, ranging from 62.5µg/ml to 1000µg/ml, were made from a stock solution and adjusted to a final volume of 100µl using phosphate buffer (0.1M, pH 7.2). The prepared samples underwent incubation at 25 °C for 10 min in the presence of 25µl of α-glucosidase. After the pre-incubation period, 1 ml of phosphate buffer (0.1M, pH 7.2) containing 37 mmol sucrose was added to initiate the reaction. The reaction combination was then further incubated for 30 min at 37 °C, with reaction termination achieved by immersing the tubes in a hot water bath for 2 min. A control tube was simultaneously kept with phosphate buffer and enzyme. Following this, 250 µl of glucose reagent was introduced to all tubes, and the resultant mixture was incubated for an additional 10 min. Absorbance measurements were performed at 510 nm utilizing a microplate reader (Erba, Lisascan) [29, 30].

$$\%\ of\ inhibition\ = \frac{control - test}{control} \times 100$$

Inhibition of glucose production in liver

HepG2 cells, obtained from NCCS (National Centre for Cell Science)-Pune, were cultured in Dulbecco's Modified Eagle's Medium (DMEM) supplemented with 10% fetal bovine serum (Invitrogen) and maintained at 37 °C with 5% CO_2 in a humidified atmosphere using a CO_2 incubator (NBS, Eppendorf) until they reached confluency. Upon reaching confluency, the cells were trypsinized using 0.025% Trypsin in PBS/0.5 mmol Ethylene diamine tetra acetic acid (EDTA) solution (Gibco, Invitrogen) for 2 min and passaged. When the cells reached 80% confluency, they were transferred to Dulbecco's Modified Eagle Medium (DMEM) without glucose along with the test sample at concentrations of 25µg/ml, 50µg/ml, and 100µg/ml from a stock solution of concentration 1 mg/ml. After 30 min, the cells were subcultured into a 24-well plate under sterile conditions. For the experimental procedure, the cells were exposed to 100nM glucagon and incubated for an additional 6 h, while an untreated control was maintained concurrently. Following incubation, the cells were extracted by the process of centrifugation at 6000 rpm for 10 min and discarded the supernatant. Subsequently, 200µl of cell lysis buffer (1M TrisHCl, 0.25M EDTA, 2M NaCl, 0.5% Triton) was added and incubated for 30 min at 4 °C. Glucose content was then determined using the glucose kit (Erba Mannheim, Germany), and absorbance measured at the wavelength 505 nm (Agilent, USA) [31].

$$Total\ Glucose\ in\ mg/dL\ = \frac{Absorbance\ of\ Test}{Absorbance\ of\ Standard} \times 100$$

$$\%\ of\ Inhibition\ = \frac{Amount\ of\ glucose\ in\ control - the\ amount\ of\ glucose\ in\ Test}{Amount\ of\ glucose\ in\ control} \times 100$$

Determination of glucose uptake assay

The L6 rat myoblast cells were procured from the NCCS (National Centre for Cell Science)-Pune. These cells were cultured in Dulbecco's Modified Eagle's Medium (DMEM) supplemented with 10% foetal bovine serum, L-glutamine, sodium bicarbonate, and an antibiotic solution comprising Penicillin (100 U/ml), Streptomycin (100 µg/ml), and Amphotericin B (2.5 µg/ml). The cell line was maintained in a 25 cm^2 tissue culture flask at 37ºC in a humidified 5% CO_2 incubator (NBS Eppendorf, Germany). For experimental procedures, cells were trypsinized using 500 µl of 0.025% Trypsin in PBS/0.5 mmol EDTA solution (Invitrogen) for 2 min and passaged to T flasks under sterile conditions. Subsequently, the cells were subcultured into a 24-well plate. Upon reaching 80% confluency, the cells were exposed to DMEM without glucose for 24 h. Samples were added to the cultured cells at final concentrations of 6.25 µg/ml, 25 µg/ml, and 100 µg/ml, prepared from a stock solution of 1 mg/ml and incubated for 24 h in DMEM containing 300 mmol glucose. A control group with elevated glucose levels remained untreated. Following incubation, cells were washed, digested, and isolated by centrifugation at 6000 rpm for 10 min. The upper layer was discarded, and 200 µl of cell lysis buffer (1M TrisHCl, 0.25M EDTA, 2M NaCl, 0.5% Triton) was added. Incubation was carried out for 30 min at 4 °C, and cellular glucose was estimated using

the high-sensitivity glucose oxidase kit method. Each experiment was carried out in triplicate, and the mean average was utilized for subsequent computations [32, 33].

$$\text{Total Glucose in mg/dL} = \frac{\text{Absorbance of Test}}{\text{Absorbance of Standard}} \times 100$$

$$\text{\% of Glucose uptake} = \frac{\text{OD of Test} - \text{OD of Control}}{\text{OD of Test}} \times 100$$

In vivo evaluation

Experimental design

A cohort of 54 adult Wistar albino rats, 8-12 w old weighing 150-200 g was acquired from Kerala Agricultural University, College of Veterinary And Animal Sciences, Mannuthy, Thrissur (Reg. No. 328/GO/Re/S/01/CPCSEA). They were maintained under the ethical committee recommendations for the study (Approval No:-PCP/IAEC/1/2021/1). Animals were housed individually in polypropylene cages to help them acclimatize to the laboratory conditions of the controlled environment at a temperature of 24-26 °C, humidity 55-60 % and photoperiod 12:12 h light and dark cycle. A commercial laboratory-balanced diet and tap water were provided *ad libitum*. The experimental setup involved the division of rats into nine groups. Initially, each rat was subjected to a single intraperitoneal injection of 110 mg/kg body weight of nicotinamide dissolved in physiological saline. Subsequently, a 15-minute interval was allowed before administering streptozotocin (STZ) into the peritoneal cavity at a dose of 60 mg/kg body weight. The STZ solution, freshly prepared in 0.1M citrate buffer at pH 4.5, was administered at a volume of 1 ml/kg body weight to induce the desired physiological response. Among the experimental group, 48 underwent peritoneal cavity injection of STZ, while 6 received saline injections and served as the control group. To mitigate early hypoglycaemic effects, rats subjected to STZ injections were provided with a 5% glucose solution for 24 h post-injection. Blood samples were retrieved from the experimental animals' tail veins 72 h after administering streptozotocin. The samples were then subjected to analysis to determine glucose levels. Animals presenting with blood glucose levels equal to or exceeding 180 mg/dl were categorized as diabetic and included in the subsequent experimental procedures. The blood glucose was estimated (mg/dl) electronically with a glucometer every 7 d in both control and experimental animal groups over 28 d [34, 35].

Biochemical assays

Following a 28 d treatment period, rats underwent a 16 h fast before being euthanized via cervical decapitation. Blood from experimental animals was obtained directly from the cardiac puncture. Subsequently, by centrifugation at 2500 rpm for 10 min, serum and plasma were separated and stored at-20 °C until they were needed for biochemical and enzyme tests [28]. Haematological parameters including haemoglobin content, glucose, and glycosylated haemoglobin, along with lipid profile components such as total cholesterol, triglycerides, High-Density Lipoproteins (HDL), Low-Density Lipoprotein (LDL), and Very Low-Density Lipoprotein (VLDL) were assessed. Additionally, serum enzyme levels, including serum glutamic-pyruvic transaminase (SGPT), serum glutamic-oxaloacetic transaminase (SGOT), and alkaline phosphatase (ALP) were measured through biochemical assays. The findings are presented as means plus or minus standard deviations (SD's). The ANOVA was conducted using Graph Pad Prism version 5.04. Tukey's multiple comparison was performed to evaluate the mean differences and the significance variations [36].

RESULTS

The study encompasses the *in silico, in vitro*, and *in vivo* analysis to validate the antidiabetic activity of newly modelled 2,3-Dihydroquinazolin-4(1H)-One derivative.

In silico evaluations

The *in silico* analysis involved eleven newly modelled 2,3-Dihydroquinazolin-4(1H)-One derivative screened for their molecular, pharmacokinetics, and pharmacodynamics properties. Six of the eleven considered molecules (QZ1, QZ2, QZ6, QZ7, QZ8, and QZ9) met the screening criteria, satisfying Lipinski's rule of 5 and possessing druggable characteristics. Thus, the molecular interaction analysis of the eight human proteins and the six ligand molecules was performed using Autodock Vina software v.1.2. To perform a comparative analysis, the standard drug molecules for each receptor were also considered for the study. Molecular docking results showed that these molecules demonstrated strong binding affinity towards key therapeutic targets associated with diabetes (table 1). Specifically, QZ9 emerged as a promising candidate with binding affinities ranging from-4.9 to-10.8 kcal/mol across various receptors (table 1). The top receptor-ligand complexes with high binding and H-bond interactions were subjected to interaction stability validation through molecular dynamic simulation and free binding energy calculation using the MMPBSA approach. The *insilico* results collectively highlight QZ9 as a promising candidate with potential antidiabetic activity, demonstrating stable interactions with key biomolecules (Peroxisome proliferator-activated receptor gamma: 4PRG and Sulfonylurea receptor-1: 6JB3) associated with T2DM (table 2) (fig. 1 and 2).

Table 1: Molecular docking result of various receptor-ligand complexes

S. No.	Ligand	Dock score (kcal/mol)-various receptor molecules (PDB ID)							
		1B2Y	2OJ9	6JB3	3DD1	5NN8	1UV5	4CDC	4PRG
1	Acarbose	-8.9	-	-	-	-8.5	-	-	-
2	Metformin	-	-4.8	-	-5.9	-	-	-	-
3	Repaglinide	-	-	-8.6	-	-	-	-	-
4	Ar-AO14418	-	-	-	-	-	-8	-	-
5	Sitagliptin	-	-	-	-	-	-	-8.6	-
6	Pioglitazone	-	-	-	-	-	-	-	-9.2
7	QZ1	-8.4	-8.6	-8.7	-8.3	-7.4	-8.7	-7.8	-9.2
8	QZ2	-8.4	-8.4	-9.2	-8	-7.7	-9.2	-9.2	-10.8
9	QZ6	-7.8	-8.3	-8.4	-7.6	-7.2	-8.1	-7.1	-8.4
10	QZ7	-8.3	-8.9	-9	-7.9	-7.8	-8.8	-9	-8.5
11	QZ8	-7.7	-7.2	-8.1	-7.4	-6.9	-9.1	-7.6	-10.4
12	QZ9	-8.1	-7.6	-8.7	-7.2	-7.6	-9	-7.2	-9.1

Dock result of multiple therapeutic targets-standard drugs and modelled molecules. RECEPTORS (PDB ID): Alpha-amylase (1B2Y), Insulin-like growth factor 1 receptor (2OJ9), Sulfonylurea receptor-1 (6JB3), Glycogen phosphorylase (3DD1), Lysosomal acid-alpha-glucosidase (5NN8), Glycogen synthase kinase-3 beta (1UV5), Dipeptidyl peptidase (4CDC), Peroxisome proliferator-activated receptor gamma (4PRG).

Table 2: Molecular docking and molecular dynamic simulation interaction result of receptor-ligand complexes

S. No.	Complex	Binding affinity (kcal/mol)	H-bond interactions in molecular docking (No: of H-bonds)	H-bond interactions in molecular dynamic simulation (No: of H-bonds)
1	4PRG_QZ9	-9.1	LYS 265, LYS 263 (2 H-bonds)	LYS 263, SER 341 (2 H-bonds)
2	6JB3_QZ9	-8.7	ASN 547, TRP 1297, ARG 1300 (3 H-bonds)	ASN 547, TRP 1297, ASN 1293 (3 H-bonds)

Molecular Docking and Molecular Dynamic simulation interaction result of Peroxisome proliferator-activated receptor gamma (4PRG) and Sulfonylurea receptor-1 (6JB3).

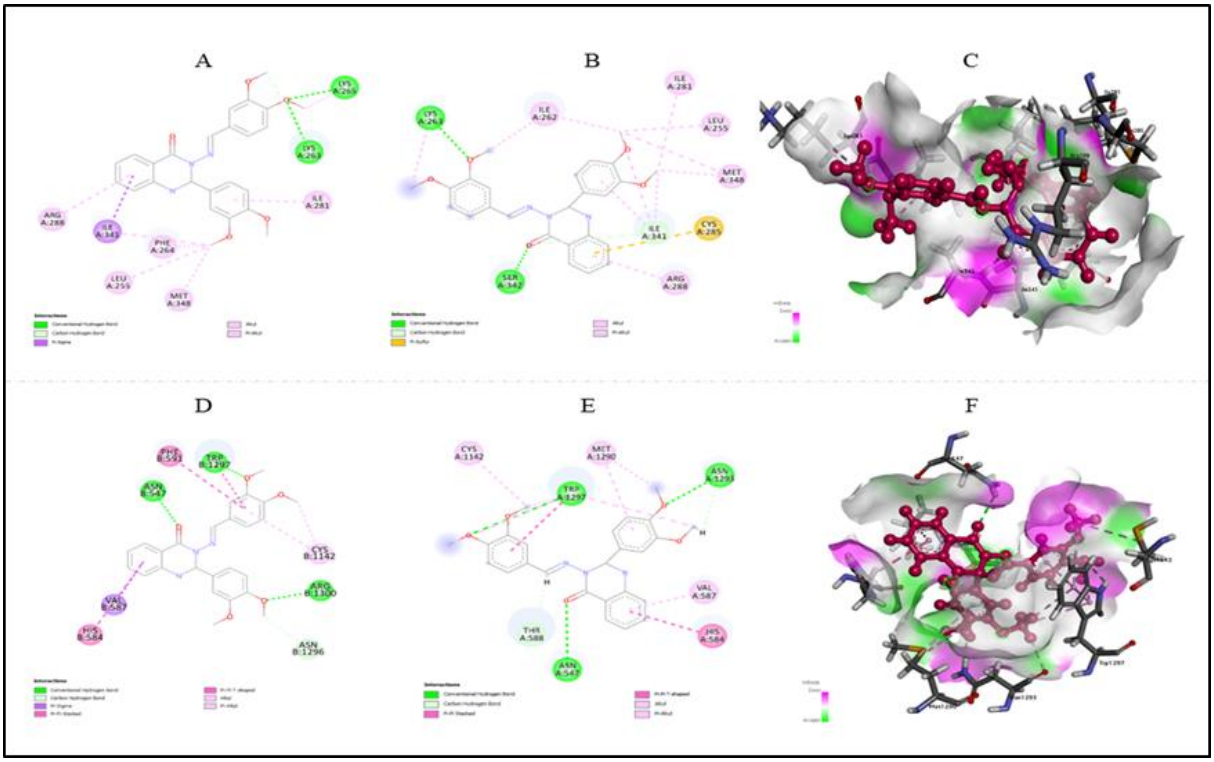

Fig. 1: *In silico* interaction analysis and stability validation results: (A) 2D interaction diagram of 4PRG_QZ9 dock complex. (B) 2D interaction diagram of 4PRG_QZ9 Molecular Dynamic Simulated complex. (C) 3D interaction diagram of 4PRG_QZ9 complex in hydrogen surface view. (D) 2D interaction diagram of 6JB3_QZ9 dock complex. (E) 2D interaction diagram of 6JB3_QZ9 Molecular Dynamic simulated complex. (F) 3D interaction diagram of 6JB3_QZ9 complex in hydrogen surface view

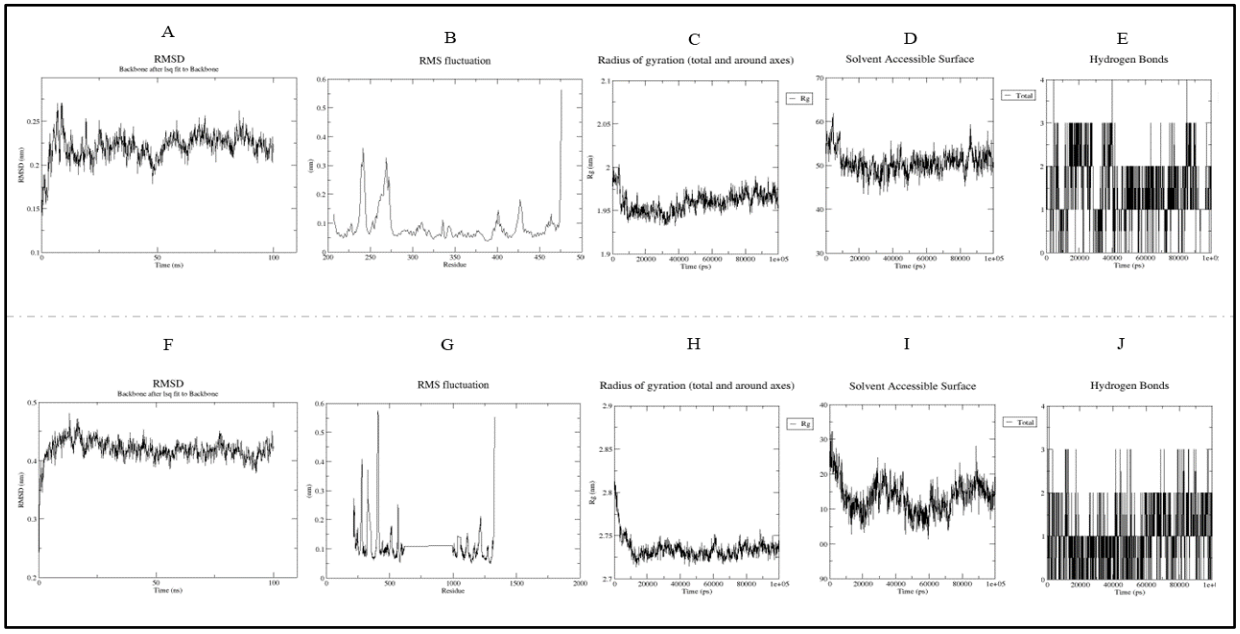

Fig. 2: Molecular dynamic simulation plots of 4PRG_QZ9 and 6JB3_QZ9 complexes – (A) Root mean **Square Deviation (RMSD), (B) Root mean square fluctuation (RMSF), (C) Radius of gyration (RoG, (D) Solvent accessible surface area (SASA) and (E) Hydrogen Bond Distribution. (F) Root** mean **Square Deviation (RMSD), (G) Root mean square fluctuation (RMSF), (H) Radius of gyration (RoG, I) Solvent accessible surface area (SASA), and (J) Hydrogen bond distribution**

In vitro evaluations

In vitro, analysis of the top-ranked molecules QZ2, QZ8, and QZ9 was performed to validate the *in silico* findings and assess the translational potential of the molecules as a therapeutic agent for T2DM. The experimental studies incorporate α-amylase inhibitory assay, α-glucosidase inhibition assay, inhibition of glucose production in the liver, and determination of *in vitro* glucose uptake assay cultured in L6 cell lines. Inhibition of α-amylase activity by Acarbose, QZ2, QZ8, and QZ9 was shown as dose-dependent from

62.5 to 1000 µg/ml concentrations (fig. 3A). At a concentration of 1000 µg/ml, Acarbose exhibited a maximum inhibition of α-amylase activity at 92.32%, while QZ2, QZ8, and QZ9 showed inhibitions of 57.33%, 52.21%, and 87.16% respectively.

The ability of Acarbose, QZ2, QZ8, and QZ9 to inhibit α-glucosidase activity was determined between 62.5 to 1000 µg/ml concentrations. All the tested molecules exhibited α-glucosidase enzyme inhibition activity in a dose-dependent fashion from 62.5 to 1000 µg/ml concentration (fig. 3B). The effect on glucose uptake and glucose inhibition was measured to assess whether QZ2, QZ8, and QZ9 contribute to the regulation of cellular glucose homeostasis. As shown (fig. 3C and 3D), QZ8 and QZ9 had increased glucose uptake and glucose inhibition in a dose-dependent manner compared to control. Maximum glucose production inhibition was observed as 62.22 % and 62.35 % at 100 µg/ml. Also, QZ8 and QZ9 equivalently increased glucose uptake from 25 to 100 µg/ml, suggesting that QZ8 and QZ9 could influence glucose homeostasis through their effect on glucose uptake and production.

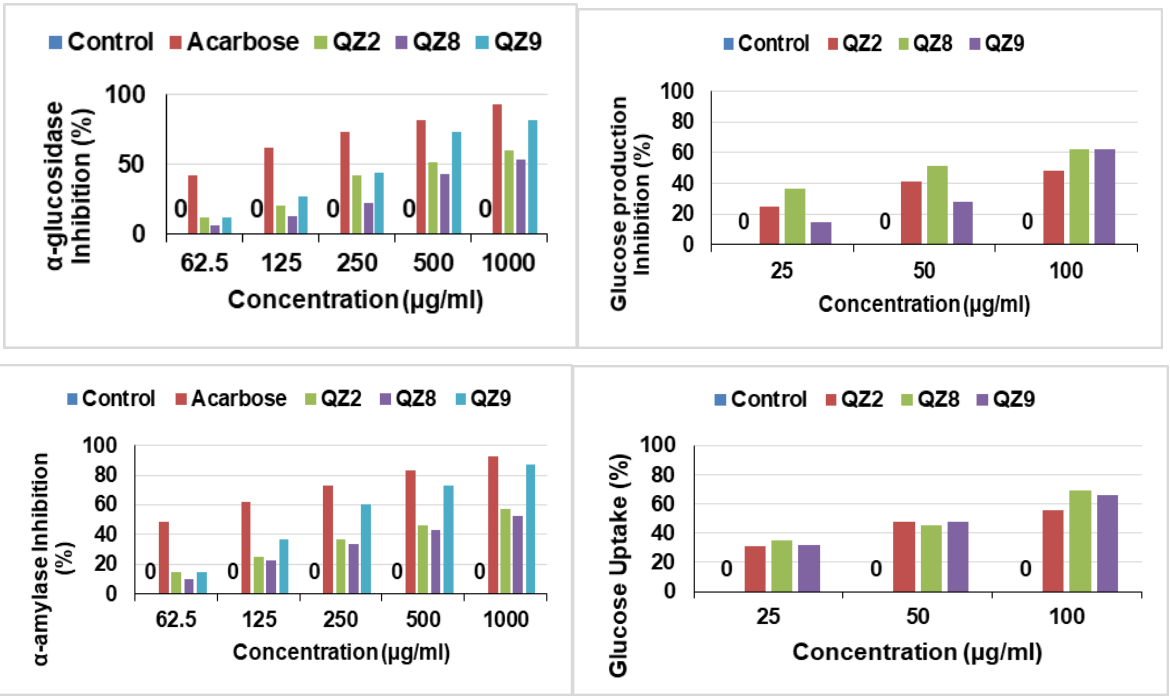

Fig. 3: (A) Alpha-amylase inhibitory activity of Acarbose, QZ2, QZ8, and QZ9. The control sample was normalized to zero. (B) Alpha-glucosidase inhibition (%) activity of Acarbose, QZ2, QZ8, and QZ9. The control sample was normalized to zero. (C) Glucose production inhibition on HepG2 cells *in vitro* by QZ2, QZ8, and QZ9. (D) Glucose uptake inhibition (%) on HepG2 cells *in vitro* by QZ2, QZ8, and QZ9

***In vivo* evaluation**

In the *in vivo* analysis, Blood glucose level quantification observed in table 3 and fig. 4A was determined at frequent intervals of 0, 7, 14, 21, and 28 d [34]. In the conducted research, it was observed that the glucose levels in group II exhibited a notable increase ($p<0.001$) in comparison to group I. However, administration of synthesized derivatives QZ2, QZ8, and QZ9 to groups III through IX resulted in a significant decrease ($p<0.001$) in blood glucose levels when contrasted with group II. Maximum blood glucose reduction was observed in group IX on the 28th d post-treatment. The biochemical analyses (table 4 and fig. 4B) revealed a significant drop in blood haemoglobin content and significant elevations in the levels of blood glucose, glycosylated haemoglobin, liver enzymes SGOT, SGPT, and ALP in diabetic-induced rats throughout the study duration. The synthesized derivatives QZ2, QZ8, and QZ9 were successful in restoring their levels at higher doses across the 28-day treatment period.

Table 3: Effect of compounds on blood glucose level

Treatment groups	Blood glucose level mg/dl				
	Days of treatment				
	0	7	14	21	28
Normal control (GP I)	114.5±1.96	118.8±2.4	111.8±4.2	113.3±3.6	111.0±5.3
Diabetic control (GP II)	223.3±14.5	230.5±2.9	236.0±4.5	234.3±3.3	232.5±2.5
Standard (GP III) Glibenclamide 2.5 mg/kg BW	261.7±17.5NS	122.3±2.9***	122.8±3.6***	126.3±4.4***	117.0±2***
Treatment with QZ2 25 mg/kg (GP IV)	248.2±8.2NS	223.5±7.8NS	211.0±2.3NS	189.0±2.3***	180.7±1.6***
Treatment with QZ2 50 mg/kg (GP V)	250.7±6.8NS	211.7±8.1NS	185.8±14.1***	197.5±3.1***	182.0±4.3***
Treatment with QZ8 25 mg/kg (GP VI)	257.7±4.7NS	176.7±2.2***	171.2±1.4***	168.5±2.0***	166.8±1.2***
Treatment with QZ8 50 mg/kg (GP VII)	248.2±4.7NS	167.5±2.3***	163.3±3.7***	157.0±1.4***	147.5±1.9***
Treatment with QZ9 25 mg/kg (GP VIII)	246.5±8.2NS	168.0±2.7***	155.8±5.0***	153.3±2.4***	130.5±1.1***
Treatment with QZ9 50 mg/kg (GP IX)	251.0±3.8NS	211.7±2.0**	153.7±2.1***	133.5±2.8***	120.0±5.1***

Post-treatment blood glucose levels in drug treatment groups compared to the diabetic control group. Statistical significance is represented as *p<0.05, **p<0.01, ***p<0.001, and NS= no significance between normal vs diabetic control and drug-treated groups and expressed as mean±SEM for n=6 in each group.

Table 4: Biochemical analysis of various blood and serum parameters post-treatment with drug groups in STZ-induced diabetes model

Treatment groups	Hb	Blood glucose	Glycosylated haemoglobin	SGOT	SGPT	ALP
Normal control	12.5±0.18	121.7±1.8	5.25±0.25	138.33±0.84	50.50±1.69	245.5±3.11
Diabetic control	10.7±0.25	243.3±8.1	13.08±0.3	251.83±5.19	71.83±2.79	280.33±5.63
Standard glibenclamide 2.5 mg/kg	12.1±0.18**	130.2±8.8***	6.42±0.33**	182.0±2.35***	51.67±1.05***	255.83±2.27**
Treatment with QZ2 25 mg/kg	11.27±0.16 NS	179.8±3.5***	8.87±0.28***	181.83±2.43***	61.6±3.59**	267.1±2.84NS
Treatment with QZ2 50 mg/kg	11.8±0.23**	169.3±2.5***	8.0±0.26***	186.83±3.03***	56.67±3.83***	256.83±1.4*
Treatment with QZ8 25 mg/kg	12.2±0.21***	160.2±0.9***	7.58±0.24***	183.283±1.6***	56.83±3.59***	251.17±4.5**
Treatment with QZ8 50 mg/kg	12.2±0.19***	151.8±1.1***	7.25±0.11***	178.67±1.02***	53.67±1.09***	245.1±2.3***
Treatment with QZ9 25 mg/kg	12.3±0.2***	151.8±2.3***	6.5±0.13***	179.17±1.01***	51.33±3.51***	239.4±19.1*
Treatment with QZ9 50 mg/kg	12.5±0.11***	121.5±2.1***	5.0±0.37***	171.33±1.2***	47.01±1.53***	245.67±3.56***

*Hb-Hemoglobin, *SGOT-Serum Glutamic Oxaloacetic Transaminase, *SGPT-Serum Glutamic Pyruvic Transaminase, *ALP-Alkaline phosphatase. Effect of various QZ2, QZ8, and QZ9 concentrations on haemoglobin, Glycosylated haemoglobin, blood glucose, and liver enzymes. Statistical significance is represented as<0.05, **p<0.01, ***p<0.001, and NS = no significance between normal vs diabetic control and drug-treated groups and expressed as mean±SEM for n=6 in each group.

An established animal model utilized in researching Type 1 diabetes mellitus is the induction of diabetes in rats via Streptozotocin (STZ) [37, 38]. It has been widely utilized to cause type 1 diabetes in experimental rat models and is well recognized for its specific cytotoxicity to pancreatic islet beta cells [39, 40]. To assess the effectiveness of various hypoglycaemic medications, glibenclamide is frequently employed as a standard antidiabetic medication in STZ-induced diabetes. This study showed that 28 d post-treatment with derivatives QZ2, QZ8, and QZ9 caused a significant drop in blood glucose at 25 and 50 mg/kg dosages in diabetic rats. All the derivatives may have an anti-diabetic impact by activating or reviving the existing pancreatic β-cells that produce more insulin. One of the potential mechanisms connecting hyperglycaemia and the vascular consequence of diabetes is increased non-enzymatic glycosylation. The excess glucose of a diabetic individual combines with haemoglobin to generate glycosylated haemoglobin such as the HbA1. In the current study, diabetic rats showed greater glycosylated haemoglobin (GyHb) serum than the normal control group, which suggested that their glycaemic management was inadequate. The total haemoglobin level increased and the GyHb level considerably dropped in diabetic rats treated with QZ2, QZ8, and QZ9, possibly due to improved glucose metabolism as suggested by Gandhi *et al.* 2012 [41].

Lipid profile analysis results that the range of blood cholesterol, HDL, and LDL reduced significantly in diabetic control when compared to the group I control (table 6 and fig. 4C). All the treatment groups restored the blood cholesterol, HDL, and LDL levels significantly showing potential pharmacological evidence *in vivo*. The increase in VLDL for diabetic control in the group I control was restored significantly in treatment groups with the highest dose of QZ9 and QZ8 than the highest dose of QZ2. The observations on the triglyceride concentration in blood reveal the efficacy of QZ2, and QZ9 to make significantly similar effects as the standard drug Glibenclamide.

Table 5: Lipid profile of blood and serum post-treatment with drug groups in STZ-induced diabetes model

Treatment groups	Total cholesterol (mg/dl)	Triglycerides (mg/dl)	HDL (mg/dl)	LDL (mg/dl)	VLDL (mg/dl)
Normal control	127.01±2.07	68.83±2.3	35±0.36	62.01±0.58	15.5±0.76
Diabetic control	99.67±1.28	125.68±1.87	20.17±0.31	31.1±0.73	25.5±0.75
Standard Glibenclamide 2.5 mg/kg bw	117.33±3.44***	75.5±1.63***	30.17±0.48***	53.33±1.74***	18.5±0.76***
Treatment with QZ2 25 mg/kg	124.68±2.73***	85.67±6.98***	27.83±0.79***	46.5±0.76***	19.5±0.76*
Treatment with QZ2 50 mg/kg	126.1±1.97***	98.67±4.4**	27.83±0.31***	47.33±1.74***	21.3±1.33*
Treatment with QZ8 25 mg/kg	124.17±1.35***	96.17±5.51**	29.17±0.31***	51.67±0.68***	21.67±0.88*
Treatment with QZ8 50 mg/kg	126.1±2.84***	106.33±3.57*	30.17±0.3***	51.67±0.56***	17.5±0.66***
Treatment with QZ9 25 mg/kg	124.67±1.75***	101.5±3.79**	30.83±0.3***	53.1±0.63***	19.0±1.77***
Treatment with QZ9 50 mg/kg	122.33±2.81***	76.33±4.18**	31.67±0.33***	55.5±0.43***	16.17±1.17***

*HDL-High-density lipoprotein, * LDL-Low-density lipoprotein, *VLDL-Very-low-density lipoprotein. Effect of various concentrations of QZ2, QZ8, and QZ9 on lipid profile. Statistical significance is represented as<0.05, **p<0.01, ***p<0.001, and NS = no significance between normal vs diabetic control and drug-treated groups. All values are expressed as mean±SEM for 6 animals in each group.

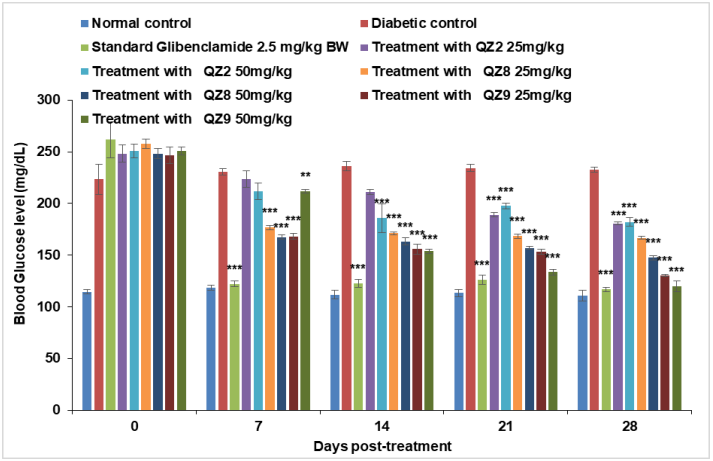

Fig. 4: (A) Post-treatment blood glucose levels in drug treatment groups compared to the diabetic control group

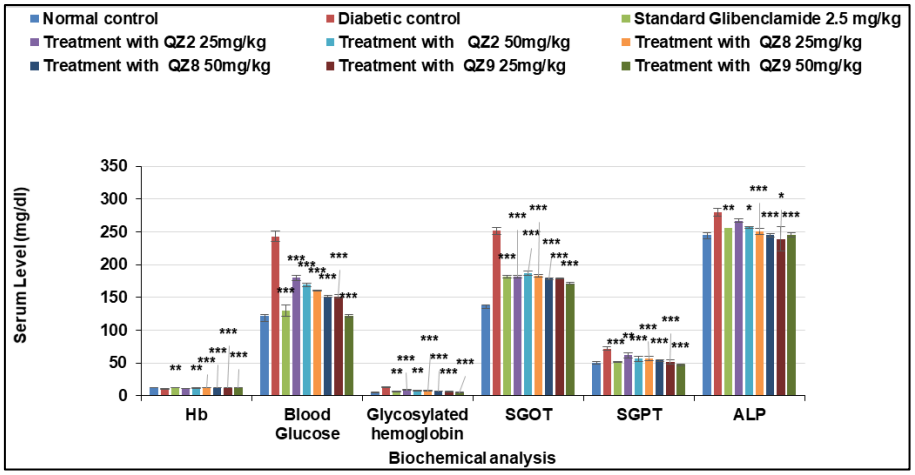

Fig. 4: (B) Biochemical analysis of various blood and serum parameters post-treatment with 25 and 50 mg/kg of QZ2, QZ8, and QZ9 in the STZ-induced diabetes model

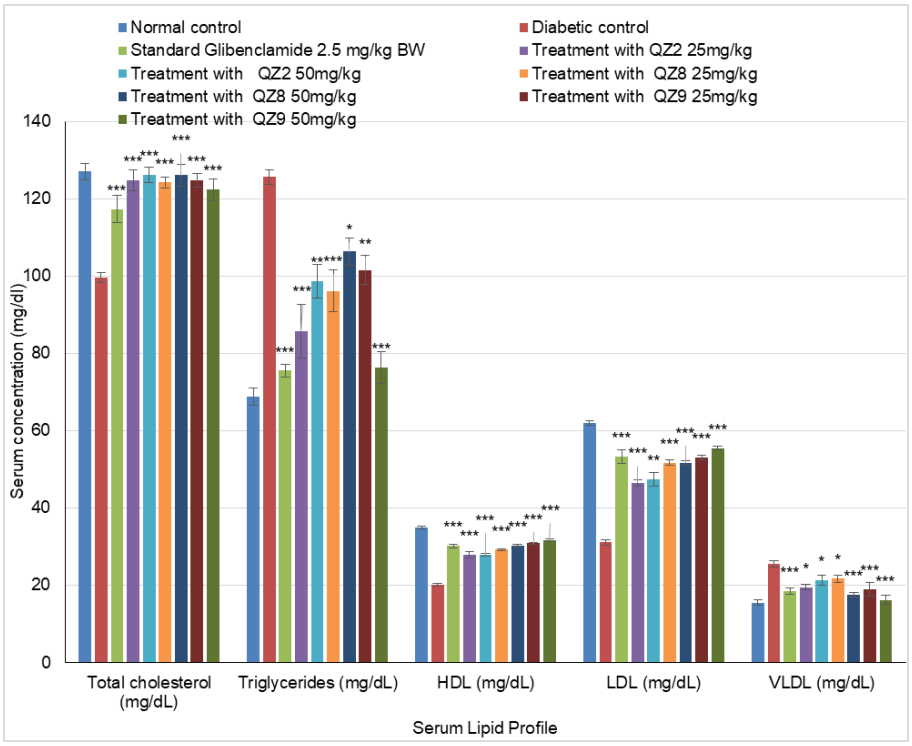

Fig. 4: (C) Lipid profile of blood and serum post-treatment with 25 and 50 mg/kg of QZ2, QZ8, and QZ9 in the STZ-induced diabetes model

The escalating incidence of atherosclerotic disease, a leading contributor to premature mortality among individuals with diabetes, has sparked considerable interest in researching plasma lipids in diabetic populations [42]. Within this investigation, serum levels of triglycerides, cholesterol, LDL cholesterol, HDL cholesterol, and VLDL cholesterol were meticulously measured. Compared to glycated LDL, which has a lower catabolic rate, glycated HDL is cleared from the bloodstream more quickly. Even with modest glycation, there is a possible chance of clearance of HDL, which can be proposed as a contributing reason to low HDL plasma levels [43]. Consequently, diabetic patients are more prone to atherosclerotic disease. The smallest lipoprotein species, HDL cholesterol, has a substantial and independent correlation with coronary heart disease (CHD). It is noteworthy that the sample exhibits approximately 20% cholesterol ester content alongside minimal levels of triglycerides.

However, the association is inverse, unlike that of LDL, with high HDL levels protecting against CHD and low HDL levels serving as a significant predictor of CHD. Diabetes has been linked to a reduction in HDL turnover. In alignment with previous research, non-enzymatic glycosylation of HDL has been identified as a contributing factor to its accelerated degradation in guinea pigs. The observed diminished levels of HDL in diabetic rats in our study potentially stem from this process [39]. Furthermore, the heightened flow of free fatty acids in the liver prompts the synthesis of VLDL, subsequently transforming LDL particles. Our investigation revealed elevated VLDL levels in individuals with type 1 diabetes, attributed to both increased production and impaired clearance. Consistent with earlier studies, a correlation was observed between elevated circulating VLDL-C and associated triglyceride levels. These alterations were linked to variations in the activity of lipoprotein lipase [44].

DISCUSSION

This study explores the therapeutic potential of 2,3-Dihydroquinazolin-4(1H)-One derivatives, particularly QZ2, QZ8,

and QZ9, as antidiabetic agents through an integrated approach combining *in silico*, *in vitro*, and *in vivo* methodologies. The research demonstrates the potential of modelled molecules, particularly QZ9, in addressing the critical challenges of Type 2 Diabetes Mellitus (T2DM), a global health crisis caused by insulin resistance or deficiency, resulting in chronic hyperglycemia and subsequent organ damage. With diabetes prevalence rising due the factors such as obesity and sedentary lifestyles, the need for novel antidiabetic agents that improve glucose regulation without severe side effects is more urgent than ever.

The quinazolinone moiety has emerged as a powerful scaffold in drug discovery, known for its diverse pharmacological properties, including antidiabetic, antioxidant, antitumor, and antimicrobial activities. Although numerous compounds with antidiabetic properties are available, there are currently no clinically approved drugs with a quinazolinone backbone for diabetes treatment, highlighting an untapped potential in this area. The versatility of the quinazolinone structure allows for the design of various derivatives with enhanced biological activities, making them ideal candidates for developing novel antidiabetic agents. This study emphasizes the therapeutic potential of these compounds, which offer a new avenue for safer and more effective diabetes management.

To explore the antidiabetic potential of quinazolinone derivatives, a series of molecules were designed and subjected to *in silico* analysis. ADMET (absorption, distribution, metabolism, excretion, and toxicity) profiling ensured that the selected derivatives, QZ2, QZ8, and QZ9, exhibited drug-like properties, including favourable pharmacokinetics and molecular characteristics that satisfy Lipinski's Rule of Five. Molecular docking studies further confirmed the binding affinity of these derivatives to key diabetes-related receptors, such as alpha-amylase (1B2Y), Insulin-like growth factor 1 receptor (2OJ9), Sulfonylurea receptor-1 (6JB3), and Peroxisome proliferator-activated receptor gamma (4PRG). Among the derivatives, QZ9 stood out, demonstrating the highest binding affinities, particularly with PPAR-γ (-9.1 kcal/mol) and SUR-1 (-8.7 kcal/mol) and it is comparable with that of standard drugs pioglitazone and repaglinide respectively. These findings strongly suggest QZ9's capability to regulate glucose metabolism and insulin production, key factors in controlling diabetes.

Molecular dynamic (MD) simulations were conducted to assess the stability of the ligand-receptor interactions under physiological conditions. The results showed that QZ9 maintained stable interactions within the binding sites of PPAR-γ and SUR-1, further validating its potential as a therapeutic agent. These *in silico* findings streamlined the subsequent experimental work, as only the most promising candidates were selected for synthesis and further biological evaluation. The computational work reduced the trial-and-error typically associated with experimental drug discovery, focusing efforts on QZ9, QZ2, and QZ8 for *in vitro* and *in vivo* analysis.

The *in vitro* evaluations of QZ2, QZ8, and QZ9 revealed their potential to inhibit α-amylase and α-glucosidase, crucial enzymes involved in carbohydrate metabolism. Additionally, QZ8 and QZ9 demonstrated significant effects on glucose uptake and inhibition of glucose production in liver cells, paralleling findings from Wang *et al.* (2020), which assessed the antidiabetic potential of natural peptides like LPLLR [45]. While LPLLR exhibited moderate enzyme inhibition, the pronounced effects of QZ9 underscore its superior potential as an antidiabetic agent. The glucose uptake and inhibition assays using L6 cell lines revealed that QZ8 and QZ9 enhanced glucose uptake in a dose-dependent manner. This is consistent with results from Aladejana *et al.* (2021), where *Helichrysum petiolare* extracts similarly influenced glucose uptake in L6 cells [46], but the effect of QZ9 was more substantial, highlighting its promising role in diabetes management.

The comparative analysis of QZ9 with previously studied molecules highlights its potential to achieve superior outcomes in antidiabetic therapies. In comparison, Khan *et al.* (2023) identified triazole-bearing bis-hydrazone derivatives as having potent inhibitory effects on both enzymes, surpassing acarbose [47]. Other studies have reported various compounds with notable anti-diabetic activity. For instance, Yousefnejad *et al.* (2023) synthesized benzo[d]imidazole-amide-1,2,3-triazole-N-arylacetamide hybrids, where more than half of the evaluated compounds inhibited α-glucosidase more effectively than Acarbose, with the most active compound being 15.3-fold more potent than the positive control [48]. Similarly, Toumi *et al.* (2021) reported that spirooxindole pyrrolidine derivatives exhibited promising activities against α-amylase, with several compounds showing higher inhibition potential than Acarbose [49]. However, when compared to these synthetic derivatives, QZ9 stands out due to its dual action on enzyme inhibition and glucose regulation, particularly in hepatic and muscular cells. This dual mechanism, as evidenced in the present study, not only positions QZ9 as a potent antidiabetic agent but also suggests its translational potential for therapeutic application in managing Type 2 Diabetes Mellitus. The combined effect of enzyme inhibition and glucose regulation by QZ9 may offer a more comprehensive approach to T2DM management compared to both synthetic drugs and natural extracts.

The *in vivo* study involving synthesized derivatives QZ2, QZ8, and QZ9 demonstrated significant antidiabetic activity in the STZ-induced diabetic rat model. The compounds showed a dose-dependent decrease in blood glucose levels, particularly evident with QZ9 at 50 mg/kg, whose efficacy was comparable to the standard drug Glibenclamide. The treatment groups also exhibited improvements in glycosylated haemoglobin (HbA1c) and liver enzyme levels, indicating enhanced glucose metabolism and reduced diabetes-related liver stress. These findings suggest that the synthesized compounds could revive pancreatic β-cells, leading to better insulin production and improved glycemic control. This glucose-lowering effect is in line with previous studies on quinazoline derivatives, which have demonstrated similar hypoglycemic and hypolipidemic properties.

Additionally, lipid profile analysis further emphasized the therapeutic potential of QZ2, QZ8, and QZ9. All treatment groups displayed a significant reduction in cholesterol, triglycerides, and LDL levels while elevating HDL concentrations, which are crucial for mitigating atherosclerotic risks in diabetic patients. These results align with studies like that of Barmak *et al.*, who observed that quinazoline derivatives not only reduced blood glucose levels but also had antihyperlipidemic effects [50]. The structural properties of these compounds, particularly the electron-withdrawing substituents, may contribute to their strong lipid-lowering and antioxidant activities. This comparison highlights the multifaceted pharmacological profile of quinazoline-based derivatives in treating both hyperglycemia and dyslipidemia, presenting them as promising candidates for further therapeutic development.

The integrated approach adopted in this study successfully identified QZ9 as a superior therapeutic agent for T2DM. Its potent enzyme inhibition, ability to regulate glucose metabolism, and favourable pharmacokinetic profile make it a promising candidate for future drug development. This study demonstrates the value of a multi-faceted approach combining *in silico*, *in vitro*, and *in vivo* evaluations to streamline the identification and validation of novel antidiabetic agents.

CONCLUSION

Type 2 Diabetes Mellitus is among the top contributors to worldwide mortality demanding the need for a potential antidiabetic lead molecule. The study employed an integrated approach to identify and suggest a druggable antidiabetic lead molecule from 2,3-Dihydroquinazolin-4(1H)-One derivative. Among the novel compounds under consideration, QZ9 exhibits high binding affinity (4PRG_QZ9--9.1 kcal/mol, 6JB3_QZ9-8.7 kcal/mol) and stable interactions with multiple T2DM-associated therapeutic targets. Experimental assays validated the inhibitory effects of QZ2, QZ8, and QZ9 on crucial enzyme activities and their potential to enhance glucose homeostasis in cellular models. *In vivo* investigations in diabetic rat models further confirmed the efficacy of QZ2, QZ8, and QZ9, showing significant reductions in blood glucose levels and beneficial effects on biochemical parameters related to diabetes complications. The results underscore the potentiality of QZ9 as a novel antidiabetic agent, warranting further exploration for clinical

application in addressing the escalating burden of diabetes mellitus on public health.

FUNDING

Nil

AUTHORS CONTRIBUTIONS

Mrs. Mincy Mathew initiated and conceptualized the research, develop the core idea and designed the computational framework. She led the data collection process and performed the experiments. Dr. Kilimozhi and Prof. Anton Smith analyzed, validated, and interpreted the results. Prof. Santhosh M. Mathews offered crucial support, provided guidance, and supervised the overall progress of the research. All authors actively participated in discussions regarding the results and collaborated in drafting and refining the final manuscript.

CONFLICTS OF INTERESTS

The authors declare no financial or other conflicts of interest in this work.

REFERENCES

1. Daina A, Michielin O, Zoete V. Swiss ADME: a free web tool to evaluate pharmacokinetics drug-likeness and medicinal chemistry friendliness of small molecules. Sci Rep. 2017 Mar 3;7:42717. doi: 10.1038/srep42717, PMID 28256516.
2. Haghighatpanah M, Nejad AS, Haghighatpanah M, Thunga G, Mallayasamy S. Factors that correlate with poor glycemic control in type 2 diabetes mellitus patients with complications. Osong Public Health Res Perspect. 2018;9(4):167-74. doi: 10.24171/j.phrp.2018.9.4.05, PMID 30159222.
3. LI M, Chi X, Wang Y, Setrerrahmane S, Xie W, XU H. Trends in insulin resistance: insights into mechanisms and therapeutic strategy. Signal Transduct Target Ther. 2022;7(1):216. doi: 10.1038/s41392-022-01073-0, PMID 35794109.
4. Tran N, Pham B, LE L. Bioactive compounds in anti-diabetic plants: from herbal medicine to modern drug discovery. Biology (Basel). 2020;9(9):1-31. doi: 10.3390/biology9090252, PMID 32872226.
5. Buggana SJ, Paturi MC, Rajendra Prasad VV. Design and synthesis of Novel 2, 3-disubstituted quinazolines: evaluation of *in vitro* anticancer activity and in silico studies. Asian J Pharm Clin Res. 2019;13(1):174-9. doi: 10.22159/ajpcr.2020.v13i1.36215.
6. Dash B, Dash S, Laloo D. Design and synthesis of 4-substituted quinazoline derivatives for their anticonvulsant and CNS depressant activities. Int J Pharm Pharm Sci. 2016;9(1):165. doi: 10.22159/ijpps.2017v9i1.15492.
7. M. WS, MA M, SA Y, G DR. Biological activity of quinazolinone derivatives: a review. Int J Curr Pharm Res. 2023;15(1):15-8.
8. Pisal P, Deodhar M, Kale A, Nigade G, Pawar S. Design synthesis docking studies and biological evaluation of 2-phenyl-3-(substituted benzo[d] thiazol-2-ylamino)-quinazoline-4(3h) one derivatives as antimicrobial agents. Int J Pharm Pharm Sci. 2018;10(10):57. doi: 10.22159/ijpps.2018v10i10.28480.
9. Daina A, Michielin O, Zoete V. Swiss ADME: a free web tool to evaluate pharmacokinetics drug-likeness and medicinal chemistry friendliness of small molecules. Sci Rep. 2017 Mar 3;7:42717. doi: 10.1038/srep42717, PMID 28256516.
10. Pires DE, Blundell TL, Ascher DB. PkCSM: predicting small molecule pharmacokinetic and toxicity properties using graph based signatures. J Med Chem. 2015 May 14;58(9):4066-72. doi: 10.1021/acs.jmedchem.5b00104, PMID 25860834.
11. Katelia R, Jauhar MM, Syaifie PH, Nugroho DW, Ramadhan D, Arda AG. In silico investigation of xanthone derivative potency in inhibiting carbonic anhydrase II (Ca Ii) using molecular docking and molecular dynamics (MD) simulation. Int J App Pharm. 2022;14(5):190-8. doi: 10.22159/ijap.2022v14i5.45388.
12. Trott O, Olson AJ. Auto dock vina: improving the speed and accuracy of docking with a new scoring function efficient optimization and multithreading. J Comput Chem. 2010;31(2):455-61. doi: 10.1002/jcc.21334, PMID 19499576.
13. Whitcomb DC, Lowe ME. Human pancreatic digestive enzymes. Dig Dis Sci. 2007;52(1):1-17. doi: 10.1007/s10620-006-9589-z, PMID 17205399.
14. Stiefel DJ, Keller PJ. Preparation and some properties of human pancreatic amylase, including a comparison with human parotid amylase. Biochim Biophys Acta. 1973;302(2):345-61. doi: 10.1016/0005-2744(73)90163-0, PMID 4699244.
15. Brissenden JE, Ullrich A, Francke U. Human chromosomal mapping of genes for insulin-like growth factors I and II and epidermal growth factor. Nature. 1984;310(5980):781-4. doi: 10.1038/310781a0, PMID 6382023.
16. Proks P, Reimann F, Green N, Gribble F, Ashcroft F. Sulfonylurea stimulation of insulin secretion. Diabetes. 2002 Dec 1;51 Suppl 3:S368-76. doi: 10.2337/diabetes.51.2007.s368, PMID 12475777.
17. Mathieu C, Dupret JM, Rodrigues Lima F. The structure and the regulation of glycogen phosphorylases in brain. Adv Neurobiol. 2019;23:125-45. doi: 10.1007/978-3-030-27480-1_4, PMID 31667807.
18. Lysosomal acid alpha-glucosidase deficiency (Pompe disease, glycogen storage disease II, acid maltase deficiency)-UpToDate.
19. Wang L, LI J, DI LJ. Glycogen synthesis and beyond a comprehensive review of GSK3 as a key regulator of metabolic pathways and a therapeutic target for treating metabolic diseases. Med Res Rev. 2022;42(2):946-82. doi: 10.1002/med.21867, PMID 34729791.
20. Rohrborn D, Wronkowitz N, Eckel J. DPP4 in diabetes. Front Immunol. 2015 Jul 27;6:386. doi: 10.3389/fimmu.2015.00386, PMID 26284071.
21. Tyagi S, Gupta P, Saini AS, Kaushal C, Sharma S. The peroxisome proliferator-activated receptor: a family of nuclear receptors role in various diseases. J Adv Pharm Technol Res. 2011;2(4):236-40. doi: 10.4103/2231-4040.90879, PMID 22247890.
22. Abraham MJ, Murtola T, Schulz R, Pall S, Smith JC, Hess B. Gromacs: high performance molecular simulations through multi-level parallelism from laptops to supercomputers. SoftwareX. 2015 Sep;1-2:19-25. doi: 10.1016/j.softx.2015.06.001.
23. Markidis S, Laure E. Solving software challenges for exascale: international conference on exascale applications and software. Lect Notes Comput Sci. 2014;8759:3–27.
24. Valdes Tresanco MS, Valdes Tresanco ME, Valiente PA, Moreno E. Gmx_MMPBSA: a new tool to perform end-state free energy calculations with GROMACS. J Chem Theory Comput. 2021 Oct 12;17(10):6281-91. doi: 10.1021/acs.jctc.1c00645, PMID 34586825.
25. Barmak A, Niknam K, Mohebbi G. Synthesis structural studies and α-glucosidase inhibitory antidiabetic and antioxidant activities of 2,3-dihydroquinazolin-4(1h) ones derived from pyrazol-4-carbaldehyde and anilines. ACS Omega. 2019;4(19):18087-99. doi: 10.1021/acsomega.9b01906, PMID 31720511.
26. Zhang J, Cheng P, MA Y, Liu J, Miao Z, Ren D. An efficient nano CuO catalyzed synthesis and biological evaluation of quinazolinone schiff base derivatives and bis-2,3-dihydroquinazolin-4(1H) ones as potent antibacterial agents against streptococcus lactis. Tetrahedron Lett. 2016 Nov 23;57(47):5271-7. doi: 10.1016/j.tetlet.2016.10.047.
27. Dabiri M, Salehi P, Otokesh S, Baghbanzadeh M, Kozehgary G, Mohammadi AA. Efficient synthesis of mono and disubstituted 2,3-dihydroquinazolin-4(1H) ones using $KAl(SO4)_2.12H_2O$ as a reusable catalyst in water and ethanol. Tetrahedron Lett. 2005 Sep 5;46(36):6123-6. doi: 10.1016/j.tetlet.2005.06.157.
28. Badolato M, Aiello F, Neamati N. 2,3-Dihydroquinazolin-4(1: H) badolato M Aiello F Neamati N 2,3-Dihydroquinazolin-4(1H) one as a privileged scaffold in drug design. RSC Adv. 2018;8(37):20894-921. doi: 10.1039/c8ra02827c, PMID 35542353.
29. Wickramaratne MN, Punchihewa JC, Wickramaratne DB. *In vitro* alpha amylase inhibitory activity of the leaf extracts of adenanthera pavonina. BMC Complement Altern Med. 2016;16(1):466. doi: 10.1186/s12906-016-1452-y, PMID 27846876.
30. Ouassou H, Zahidi T, Bouknana S, Bouhrim M, Mekhfi H, Ziyyat A. Inhibition of α-glucosidase intestinal glucose absorption and antidiabetic properties by caralluma europaea. Evid Based Complement Alternat Med. 2018 Aug 29;2018:9589472. doi: 10.1155/2018/9589472, PMID 30228829.

31. Guo L, Zheng X, Liu J, Yin Z. Geniposide suppresses hepatic glucose production via AMPK in hepG2 cells. Biol Pharm Bull. 2016;39(4):484-91. doi: 10.1248/bpb.b15-00591, PMID 26830672.
32. Yamamoto N, Ueda Wakagi M, Sato T, Kawasaki K, Sawada K, Kawabata K. measurement of glucose uptake in cultured cells. Curr Protoc Pharmacol. 2015;71(1):12.14.1-12.14.26. doi: 10.1002/0471141755.ph1214s71, PMID 26646194.
33. Zhou F, Furuhashi K, Son MJ, Toyozaki M, Yoshizawa F, Miura Y. Antidiabetic effect of enterolactone in cultured muscle cells and in type 2 diabetic model db/db mice. Cytotechnology. 2017;69(3):493-502. doi: 10.1007/s10616-016-9965-2, PMID 27000262.
34. Asagba SO, Kadiri HE, Ezedom T. Biochemical changes in diabetic rats treated with ethanolic extract of Chysophyllum albidum fruit skin. The Journal of Basic and Applied Zoology. 2019;80(1). doi: 10.1186/s41936-019-0118-y.
35. Poovitha S, Parani M. *In vitro* and *in vivo* α-amylase and α-glucosidase inhibiting activities of the protein extracts from two varieties of bitter gourd (Momordica charantia L.). BMC Complement Altern Med. 2016;16 Suppl 1:185. doi: 10.1186/s12906-016-1085-1, PMID 27454418.
36. Gopal V, Mandal V, Tangjang S, Mandal SC. Serum biochemical histopathology and SEM analyses of the effects of the Indian traditional herb wattakaka volubilis leaf extract on wistar male rats. J Pharmacopuncture. 2014;17(1):13-9. doi: 10.3831/KPI.2014.17.002, PMID 25780685.
37. Ozougwu O. The pathogenesis and pathophysiology of type 1 and type 2 diabetes mellitus. J Physiol Pathophysiol. 2013;4(4):46-57. doi: 10.5897/JPAP2013.0001.
38. Bell RH, Hye RJ. Animal models of diabetes mellitus: physiology and pathology. J Surg Res. 1983;35(5):433-60. doi: 10.1016/0022-4804(83)90034-3, PMID 6314046.
39. Lenzen S. The mechanisms of alloxan and streptozotocin-induced diabetes. Diabetologia. 2008;51(2):216-26. doi: 10.1007/s00125-007-0886-7, PMID 18087688.
40. Tomlinson KC, Gardiner SM, Hebden RA, Bennett T. Functional consequences of streptozotocin-induced diabetes mellitus with particular reference to the cardiovascular system. Pharmacol Rev. 1992;44(1):103-50. PMID 1557425.
41. Gandhi GR, Sasikumar P. Antidiabetic effect of Merremia emarginata Burm. F. in streptozotocin induced diabetic rats. Asian Pac J Trop Biomed. 2012;2(4):281-6. doi: 10.1016/S2221-1691(12)60023-9, PMID 23569914.
42. Andallu B, Vinay Kumar AV, Varadacharyulu NCh. Lipid abnormalities in streptozotocin diabetes: amelioration by Morus indica L. cv suguna leaves. Int J Diabetes Dev Ctries. 2009;29(3):123-8. doi: 10.4103/0973-3930.54289, PMID 20165649.
43. Hollenbeck CB, Chen YD, Greenfield MS, Lardinois CK, Reaven GM. Reduced plasma high-density lipoprotein cholesterol concentrations need not increase when hyperglycemia is controlled with insulin in noninsulin-dependent diabetes mellitus. J Clin Endocrinol Metab. 1986;62(3):605-8.
44. Pandhare RB, Sangameswaran B, Mohite PB, Khanage SG. Anti-hyperglycaemic and lipid-lowering potential of Adenanthera pavonina Linn. in streptozotocin-induced diabetic rats. Orient Pharm Exp Med. 2012;12(3):197-203. doi: 10.1007/s13596-012-0074-2, PMID 22924034.
45. Wang J, WU T, Fang L, Liu C, Liu X, Li H. Anti-diabetic effect by walnut (Juglans mandshurica Maxim.) derived peptide LPLLR through inhibiting α-glucosidase and α-amylase and alleviating insulin resistance of hepatic HepG2 cells. J Funct Foods. 2020 Jun 1;69:103944. doi: 10.1016/j.jff.2020.103944.
46. Aladejana AE, Bradley G, Afolayan AJ. *In vitro* evaluation of the antidiabetic potential of Helichrysum petiolare hilliard and B. L. Burtt using HepG2. 1240; C3A and L6 cell lines. F1000 Research. 2021;9.
47. Khan I, Rehman W, Rahim F, Hussain R, Khan S, Rasheed L. Synthesis and *in vitro* α-amylase and α-glucosidase dual inhibitory activities of 1,2,4-triazole-bearing bis-hydrazone derivatives and their molecular docking study. ACS Omega. 2023;8(25):22508-22. doi: 10.1021/acsomega.3c00702, PMID 37396210.
48. Yousefnejad F, Mohammadi Moghadam Goozali M, Sayahi MH, Halimi M, Moazzam A, Mohammadi Khanaposhtani M. Design synthesis *in vitro* and in silico evaluations of benzo[d]imidazole-amide-1,2,3-triazole-N-arylacetamide hybrids as new antidiabetic agents targeting α-glucosidase. Sci Rep. 2023;13(1):12397. doi: 10.1038/s41598-023-39424-8, PMID 37524733.
49. Toumi A, Boudriga S, Hamden K, Sobeh M, Cheurfa M, Askri M. Synthesis antidiabetic activity and molecular docking study of rhodanine substitued spirooxindole pyrrolidine derivatives as novel α-amylase inhibitors. Bioorg Chem. 2021;106:104507. doi: 10.1016/j.bioorg.2020.104507, PMID 33288322.
50. Barmak A, Niknam K, Mohebbi G. Synthesis structural studies and α-glucosidase inhibitory antidiabetic and antioxidant activities of 2,3-dihydroquinazolin-4(1H) ones derived from pyrazol-4-carbaldehyde and anilines. ACS Omega. 2019;4(19):18087-99. doi: 10.1021/acsomega.9b01906, PMID 31720511.